Kerr Spatiotemporal Self-Focusing in a Planar Glass Waveguide

H. S. Eisenberg, R. Morandotti,* and Y. Silberberg
Department of Physics of Complex Systems, Weizmann Institute of Science, Rehovot, Israel, 76100

S. Bar-Ad
School of Physics and Astronomy, Tel-Aviv University, Ramat Aviv, Tel-Aviv, Israel, 69978

D. Ross and J. S. Aitchison
Department of Electronics and Electrical Engineering, University of Glasgow, Glasgow, Scotland, G12 8QQ
(Received 1 January 2001; published 6 July 2001)

We observed simultaneous focusing in both space and time for light pulses propagating in a planar waveguide. In particular, 60 fs pulses with a width of 170 μm were injected into a planar glass waveguide in the anomalous dispersion regime. Output pulses as short as 30 fs and as narrow as 20 μm were measured. The results suggest that multiphoton absorption and intrapulse stimulated Raman scattering arrest the spatiotemporal contraction. The results were compared to the pulse evolution in zero and normal dispersion regimes and were shown to be significantly different. All of the experimental results were reproduced by a numerical model.

DOI: 10.1103/PhysRevLett.87.043902 PACS numbers: 42.65.Tg, 42.65.Dr, 42.65.Re, 42.65.Sf

The propagation of intense ultrashort light pulses has received a lot of attention over the past decade. It is influenced by the interplay of various physical mechanisms, the most important being diffraction, material dispersion, the nonlinear Kerr effect, and nonlinear absorption [1]. One of the most intriguing cases is when diffraction and dispersion have the same magnitude. In the linear regime this results in a pulse that expands uniformly in space and time. At high light intensity the Kerr nonlinearity simultaneously compensates for both effects, leading to spatiotemporal contraction and possibly to the formation of optical light bullets [2]. Such a case occurs in materials with a positive Kerr coefficient, anomalous dispersion, and where the pulse dispersion and diffraction lengths are equal.

Basic analysis of the propagation of multidimensional pulses, involving the slowly varying envelope approximation, predicts instability [2]. Such pulses are categorized as "1 + 2" and "1 + 3" cases, depending on whether diffraction is limited to one dimension, as in a planar waveguide, or to two, as in a bulk medium. A pulse having power beyond a critical value is predicted to contract to a singular solution. However, such mathematical collapse is usually avoided in experiments because of other effects which become significant, e.g., higher order nonlinearities such as multiphoton absorption [3] and saturation of the Kerr nonlinearity [4]. Light bullets are solitary light pulses that propagate while retaining their shape in all dimensions. They are a combination of the well-known spatial and temporal solitons.

Recently, a few experiments attempted to demonstrate simultaneous spatiotemporal focusing. Nevertheless, all the nonlinearities used were other than Kerr. Liu *et al.* [5] used the cascading of quadratic nonlinearity to create a bound pair of fundamental and second harmonic pulses, copropagating while balancing each other's spatiotemporal shape. In another experiment [6], the balancing of normal dispersion by its higher orders and the Kerr nonlinearity was shown to form stable three-dimensional pulses in a bulk media. Pulse splitting in the normal dispersion regime, where self-phase-modulation broadens the pulse temporally, was also demonstrated experimentally [7].

In this paper we study experimentally the propagation of intense ultrashort pulses in the 1 + 2 case in a planar glass waveguide, where the Kerr nonlinearity is predominant. We compare the nonlinear behavior in the different regimes of anomalous, zero, and normal dispersion [8]. The pulses focus simultaneously in space and time only in the anomalous case. Nevertheless, we do not observe the predicted catastrophic collapse [2]. In fact, beyond a certain power at which the spatial and temporal profiles are the narrowest, the pulses start to expand. We present numerical studies showing that the main causes for this behavior are multiphoton absorption [3] and intrapulse Raman scattering [9,10]. Based on this model, we believe that, after the pulse reaches its minimal size, it propagates in a way that resembles the propagation of light bullets. However, our results also suggest that such pulses cannot propagate indefinitely, since the same effects that arrest their collapse eventually cause their expansion. This is the first time that spatiotemporal focusing has been experimentally observed in a Kerr medium.

In the experiment we coupled transform limited 60 fs pulses, with peak powers up to 20 MW, from a Spectra Physics OPA 800 optical parametric amplifier, into planar glass waveguides. We used a combination of microscope objective and cylindrical lenses to achieve an elliptical beam, about 170-μm wide, with a flat phase front at the input facet of the sample. This combination also enables matching of the beam size, and thereby the diffraction length, to the dispersion length in the glass. The

single-mode waveguide was 3-cm long, consisting of a 4-μm-thick germanium-boron doped silica slab waveguide deposited by flame hydrolysis deposition on an oxidized silicon wafer with a 14-μm-thick layer of SiO_2. The output facet of the sample was imaged onto an infrared camera. A portion of the beam was directed to a spectrometer. Another portion of the beam was directed to a noncollinear autocorrelator. The 100-μm-thick BBO nonlinear crystal used in our autocorrelator enables accurate measurement of pulse durations down to 10 fs. The glass in the optical path to the autocorrelator introduced a systematic error to the pulse width measurements, which we estimate to be smaller than 10 fs. An aperture, placed in an image plane of the output facet, allowed temporal and spectral characterizations of the central part of the output beam. We repeated the experiment at three different wavelengths, 1.52 μm (anomalous dispersion), 1.30 μm (zero dispersion), and 1.04 μm (normal dispersion).

The results for the anomalous dispersion case, with the laser tuned to 1.52 μm, are shown in Fig. 1. Figure 1(a) shows the beam spatial profile at the output facet for different values of power. As the power of the incoming beam is increased, the beam width first contracts to about 20 μm, then remains nearly unchanged as the power is increased. Eventually, the beam slightly broadens while breaking up into filaments which broaden and merge. The corresponding autocorrelation traces [Fig. 1(b)] also show a contraction by a factor of nearly 2. It is important to note that the temporal profile and the spatial cross section evolve simultaneously, reaching their minimum values at the same power. This can be clearly seen in Fig. 2, where the beam parameters are plotted as a function of the peak power. Both parameters exhibit a shallow minimum at about 600 kW. This value should be compared with a value of 160 kW for which collapse is theoretically predicted for the parameters of our experiment [2].

The pulse does not collapse, as would be expected for a pure Kerr nonlinearity and anomalous dispersion model. As we discuss below, numerical simulations suggest that this is due to the significance of multiphoton absorption and stimulated Raman scattering (SRS). These processes account for the higher than expected power required to induce spatiotemporal contraction, as well as for the eventual expansion of the pulses. We attribute the filamentation of the beam at high powers to instability due to imperfections in the input beam profile. Simulations suggest that, even with a smoother profile, filamentation occurs at high power because of instabilities induced by nonlinear absorption [11].

We next compare the pulse evolution for three dispersion regimes. The measured spatial and temporal widths for the three different wavelengths are presented in Figs. 2(a) and 2(b), respectively. Spatial width data is presented only for input powers below which filamentation does not occur. Evidently, spatial self-focusing is observed in all three cases, but temporal contraction occurs only in the case of anomalous dispersion. Rather than becoming shorter, a significant increase of the pulse duration is observed

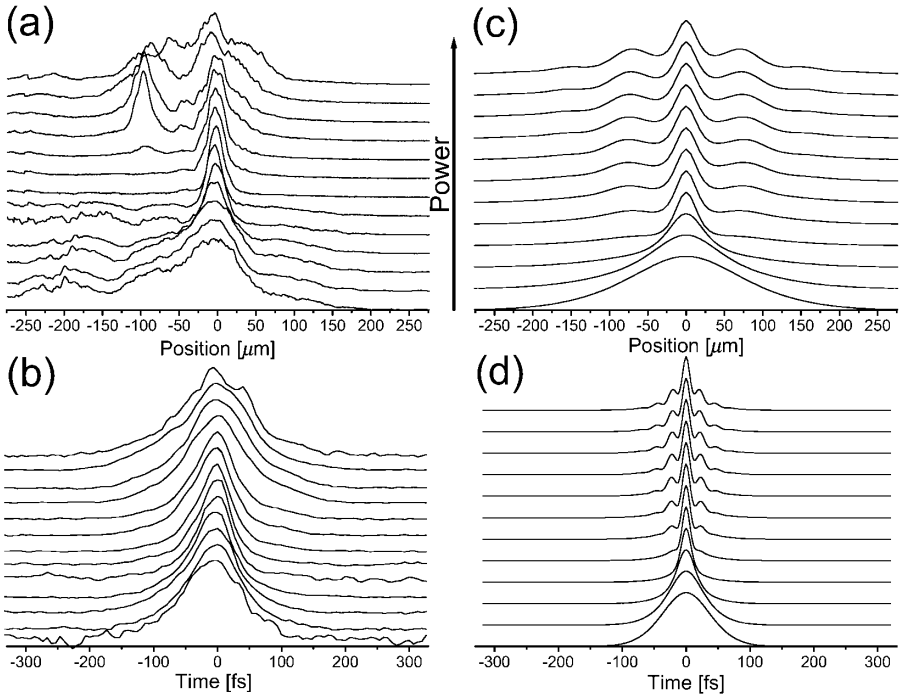

FIG. 1. Normalized (a) spatial profiles and (b) temporal autocorrelation traces of the light pulses emerging from the sample. The profiles are arranged so that results at higher input powers are plotted sequentially upwards. Spatial and temporal contraction are obtained simultaneously for peak powers of 600 kW. For a comparison with the numerical results, see (c) for spatial profiles and (d) for on-axis temporal autocorrelation traces.

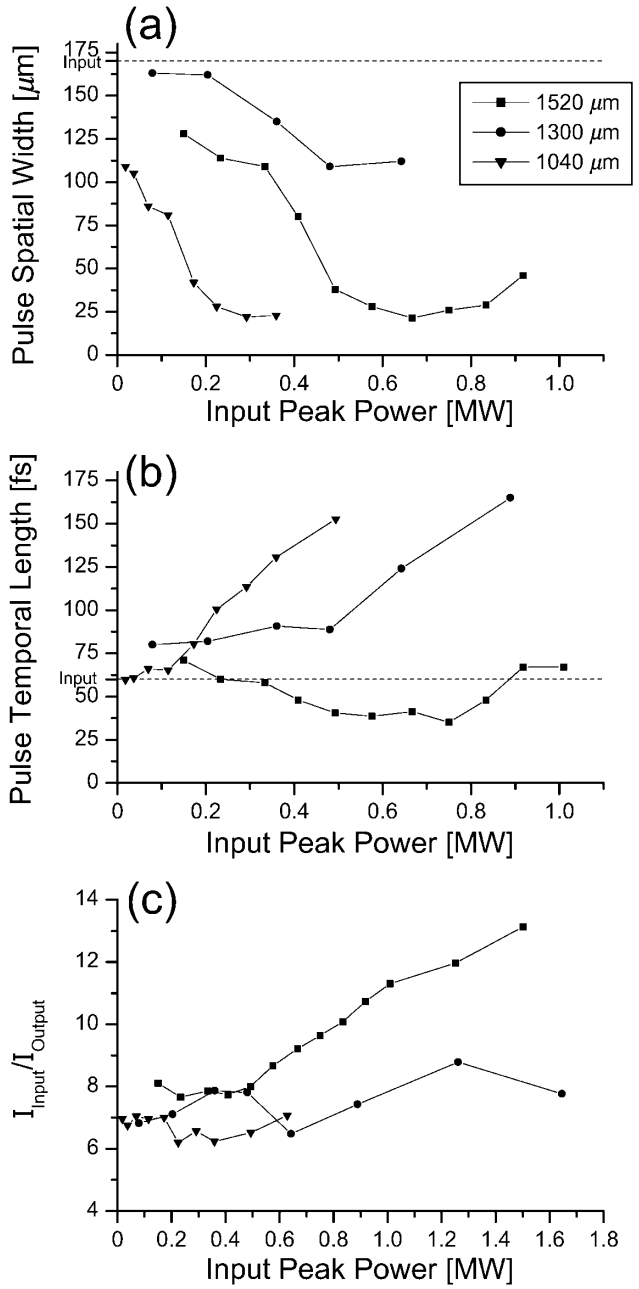

FIG. 2. A comparison of the output pulses (a) spatial and (b) temporal widths in the three different dispersion regimes. The pulses contract temporally only in the anomalous dispersion regime (squares), while in the zero (circles) and normal (triangles) dispersion regimes there is nonlinear temporal broadening. In the zero dispersion case, temporal broadening occurs only after self-phase-modulation creates enough spectrum at wavelengths far away from the zero dispersion wavelength. (c) Losses in the sample. Intensities high enough for nonlinear absorption are achieved only in the case of anomalous dispersion.

for normal dispersion [12]. For zero dispersion, no pulse broadening occurs initially, as expected. Yet, as the pulse spectrum expands through self-phase-modulation at higher powers (see Fig. 3 below), most of the energy in the pulse is pushed out of the zero dispersion regime, and the pulse begins to broaden. As a result, the contraction is effectively one dimensional in the normal and zero dispersion regimes, while it is two dimensional in the anomalous dispersion regime. The higher power which is needed to achieve contraction in the anomalous dispersion regime is consistent with its higher dimensionality [2]. Simultaneous spatiotemporal contraction results in higher intensities, leading to stronger multiphoton absorption and also contributes to the increased power requirement. Indeed, as shown in Fig. 2(c), we observed significant nonlinear loss only in the anomalous case.

As seen in Figs. 2(a) and 2(b), there is an asymmetry between the compression achieved in space and in time. We attribute it to the wavelength limit on spatial and temporal focusing. The spot-size limit for focusing is about one wavelength. The minimal beam width that was observed in our experiment is about 20 times wider than the wavelength in the medium. On the other hand, in the time domain the minimal pulse length of 30 fs contains only about six optical cycles. Near the wavelength limit, higher orders of dispersion become important and affect the rate of compression.

Figure 3 shows the measured spectra as a function of increasing power. The spectra for anomalous, zero and normal dispersion are plotted in Figs. 3(a), 3(b), and 3(c), respectively. In all three cases the spectra at low power closely resemble those of the respective input pulses, while at high power they broaden considerably through self-phase-modulation. In the anomalous dispersion regime

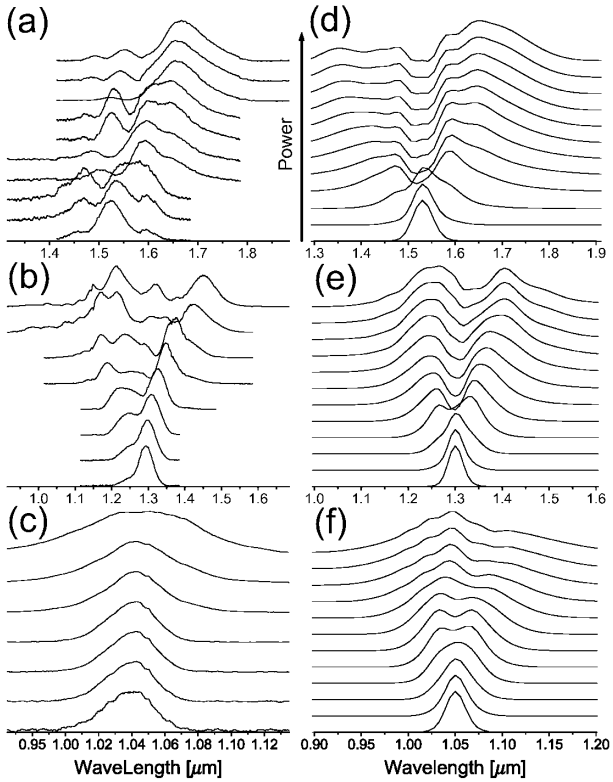

FIG. 3. Spectra recorded for (a) anomalous, (b) zero, and (c) normal dispersion for increasing input power. Numerical results are compared in (d), (e), and (f), respectively.

the broadening is accompanied by a pronounced Raman self-frequency shift towards longer wavelengths [13,14]. In contrast, near zero dispersion [Fig. 3(b)] a Stokes Raman scattering wing appears together with an anti-Stokes component [15]. The generation of anti-Stokes frequencies is unique to this regime because all three frequencies (input signal, Stokes, and anti-Stokes) propagate with nearly the same group velocity. In the case of normal dispersion [Fig. 3(c)] the spectra are characterized by a symmetric broadening. SRS is absent due to mismatch between the delayed nonlinear polarization which is mainly behind the pulse and the long wavelength Raman frequencies that travel faster towards their front. The data presented in Fig. 3(a) was taken with a longer 5-cm sample, but this has only a small effect on the emerging spectra.

We compare these experimental results to numerical simulations. The numerical model is based on a modified nonlinear Schrödinger equation for the field amplitude E:

$$i\frac{\partial E}{\partial z} = -\frac{1}{2k}\frac{\partial^2 E}{\partial x^2} + \frac{1}{2}\beta_2\frac{\partial^2 E}{\partial t^2} + k\frac{n_2}{n_0}E\int_0^\infty R(t')|E(t-t')|^2\,dt' - i\frac{\alpha_n}{2}|E|^{2(n-1)}E\,.$$

In this equation, k is the vacuum wave number, β_2 is the dispersion parameter, n_2 is the Kerr coefficient, and α_n is an n-photon absorption parameter. $R(t) = f_{\text{inst}}\delta(t) + f_{\text{delay}}h_R(t)$ includes the instantaneous and delayed parts of the Kerr nonlinearity. The delayed nonlinear response is known to approximate the Raman effect in silica and may be written in the form $h_R(t) = \exp(-t/\tau_2)\sin(t/\tau_1)$ [9], where τ_1 and τ_2 are the nonlinear polarization oscillations and decay typical time scales, respectively. The last term in the equation describes multiphoton absorption [3]. We chose $n = 6$ because six-photon absorption is expected to be the dominant term in glass for 1520-nm light. The model reproduced our experimental results quite well. First, we obtained spatial self-focusing in all three regimes, as expected, while in the time domain there is contraction only for the anomalous dispersion case. The zero and normal dispersion cases result in temporal broadening and eventually in pulse splitting, as predicted numerically [16] and recently observed experimentally [7]. Many features of the experiments were reproduced by the simulations. In particular, we obtained all the spectral features: self-frequency shift and spectral broadening in the anomalous case, Stokes and anti-Stokes scattering in the zero dispersion case and only spectral broadening due to self-phase-modulation in the normal case. The spatial and temporal evolution for the anomalous case is presented in Figs. 1(c) and 1(d), while the spectral evolution for all three cases is presented in Fig. 3.

In conclusion, we demonstrated for the first time simultaneous spatial and temporal focusing of ultrashort pulses via the Kerr effect in a glass planar waveguide in the anomalous dispersion regime. The narrow pulse which is formed (20 μm $\times$ 30 fs) seems to be stable for a range of input intensities. Catastrophic collapse is avoided probably due to multiphoton absorption; however, no damage was observed. Our numerical results show that, after a transient length of about 1 cm, the pulse propagates with an almost stable spatiotemporal profile, resembling a light bullet. We compared the evolution in the anomalous dispersion regime to that in the zero and normal regimes. Numerical simulations agree well with our observations, suggesting that we have a good understanding of the dominant processes in these experiments.

We acknowledge the EPSRC in the United Kingdom and the Ministry of Science and Technology in Israel for their financial support of this project.

*Also with the Department of Electronics and Electrical Engineering, University of Glasgow, Glasgow, Scotland, G12 8QQ.

[1] R. W. Boyd, *Nonlinear Optics* (Academic Press, San Diego, 1992).
[2] Y. Silberberg, Opt. Lett. **15**, 1282 (1990).
[3] A. L. Dyshko, V. N. Lugovoi, and A. M. Prokhorov, Sov. Phys. JETP **34**, 1235 (1972).
[4] J. H. Marburger and E. Dawes, Phys. Rev. Lett. **21**, 556 (1968).
[5] X. Liu, L. J. Qian, and F. W. Wise, Phys. Rev. Lett. **82**, 4631 (1999).
[6] I. G. Koprinkov, A. Suda, P. Wang, and K. Midorikawa, Phys. Rev. Lett. **84**, 3847 (2000).
[7] J. K. Ranka, R. W. Schirmer, and A. L. Gaeta, Phys. Rev. Lett. **77**, 3783 (1996).
[8] A. Hasegawa and F. Tappert, Appl. Phys. Lett. **23**, 142 (1973); A. Hasegawa and F. Tappert, Appl. Phys. Lett. **23**, 171 (1973).
[9] K. J. Blow and D. Wood, IEEE J. Quantum Electron. **25**, 2665 (1989).
[10] R. J. Hawkins and C. R. Menyuk, Opt. Lett. **18**, 1999 (1993).
[11] Y. Silberberg, Opt. Lett. **15**, 1005 (1990).
[12] G. P. Agrawal, *Nonlinear Fiber Optics* (Academic Press, San Diego, 1995).
[13] F. M. Mitschke and L. F. Mollenauer, Opt. Lett. **11**, 659 (1986).
[14] J. P. Gordon, Opt. Lett. **11**, 662 (1986).
[15] P. Beaud, W. Hodel, B. Zysset, and H. P. Weber, IEEE J. Quantum Electron. **QE–23**, 1938 (1987).
[16] P. Chernev and V. Petrov, Opt. Lett. **17**, 172 (1992); J. E. Rothenberg, Opt. Lett. **17**, 583 (1992).